Macromolecules

pubs.acs.org/Macromolecules

Article

Roadmap to Design Mechanically Robust Copolymer Hydrogels Naturally Cross-Linked by Hydrogen Bonds

Cagla Erkoc, Erol Yildirim, Mine Yurtsever,* and Oguz Okay*

Cite This: *Macromolecules* 2022, 55, 10576−10589

Read Online

ACCESS | Metrics & More | Article Recommendations | Supporting Information

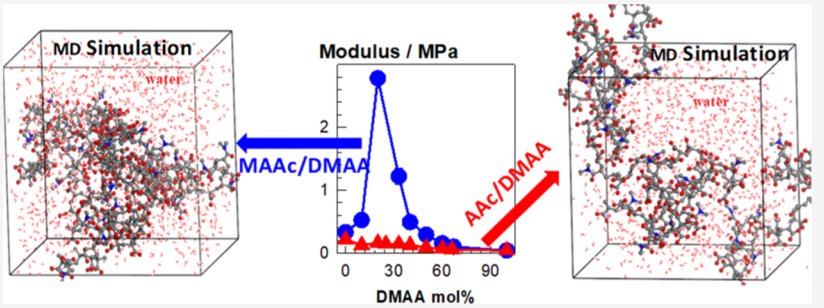

ABSTRACT: Although several mechanically strong physical hydrogels bearing H-bond donor and acceptor groups have been reported over the past years, the effect of the complex interplay between competing interactions on the mechanical strength of H-bonded hydrogels remains a challenge. We present here the mechanical properties of six different copolymer hydrogels formed under identical conditions. Methacrylic acid (MAAc), acrylic acid (AAc), *N*,*N*-dimethylacrylamide (DMAA), 1-vinylimidazole (NVI), *N*-vinyl pyrrolidone (NVP), and acrylamide (AAm) monomers were copolymerized to form MAAc/DMAA, AAc/DMAA, AAc/NVI, MAAc/NVI, MAAc/NVP, and AAm/NVP hydrogels, respectively, at various molar ratios in the presence of 60 wt % water. The hydrophobicity of the monomers and the competing interactions between the copolymer chains and copolymer−water were quantitatively elucidated by the all-atom MD simulations in the explicit water, density functional theory calculations, and molecular descriptors by remaining faithful to the experimental compositions. Young's modulus of the hydrogels could be varied between 10^{-1} and 10^{1} MPa by changing the type and molar ratio of the comonomers. AAc/DMAA and AAm/NVP hydrogels exhibit the lowest moduli, 0.11 ± 0.05 and 0.20 ± 0.04 MPa, respectively, over all comonomer compositions, while for all other comonomer pairs, the resulting hydrogels assume a maximum modulus at a critical composition. MAAc and NVI are the most effective major and minor components, respectively, to generate copolymer hydrogels with a high modulus and strength. The crucial factors determining the mechanical performance of the copolymer hydrogels are the hydrophobicity of the major copolymer component, ionic H-bonds, formation of strong H-bonded nanoaggregates, and stronger and higher inter-chain H-bonding and hence electrostatic interactions.

INTRODUCTION

A significant development has been achieved in the past 2 decades in designing synthetic hydrogels with extraordinary mechanical properties comparable to biological tissues.[1−11] The new-generation hydrogels generally possess strong and weak cross-link junctions creating an effective energy dissipation mechanism and providing them chain dynamics and hence a high toughness. For instance, double-network hydrogels composed of interpenetrating brittle and ductile networks or single-network hydrogels formed by both chemical and physical cross-links exhibit remarkable mechanical performances.[2,3,12] Cooperative H-bonding, hydrophobic, ionic, metal−ligand, $\pi-\pi$ stacking interactions, and crystalline domains have also been utilized to create dynamic physical cross-links in mechanically robust hydrogels with self-healing ability.[13−18]

Research on high-toughness physical hydrogels over the past years has focused on the preparation of hydrogels by a simple one-pot reaction method, namely, free-radical copolymerization of H-bond donor and acceptor monomers in aqueous solutions without a chemical cross-linker.[16,19−25] Because the strength of H-bonds between hydrophilic polymer chains in water is much weaker than between water molecules, self-complementary dual or multiple H-bonding interactions are created in hydrogels, and their water content is reduced to a moderate level (20−80 wt %).[20−25] To further amplify the H-bonding interactions, hydrophobic segments are incorporated into the hydrophilic polymers.[22,26−29] For instance, copoly-

Received: July 15, 2022
Revised: October 29, 2022
Published: November 25, 2022

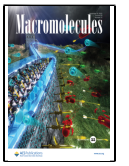

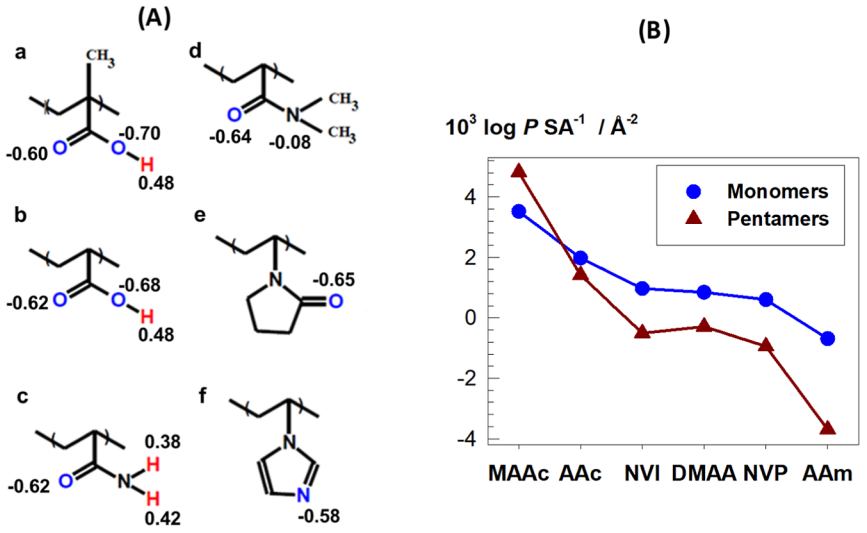

Figure 1. (A) Chemical structure of the repeating units: (a) MAAc, (b) AAc, (c) AAm, (d) DMAA, (e) NVP, and (f) NVI. The ESP charges on H-bond donor and acceptor atoms are shown. The H-bond donors and acceptors are red and blue in color, respectively. (B) Log *P* values for the monomers and pentamers normalized with respect to the solvent-accessible surface area (SA).

merization of *N*,*N*-dimethylacrylamide (DMAA) and methacrylic acid (MAAc) without a chemical cross-linker in aqueous solutions at a water content of 70 wt % results in hydrogels with a Young's modulus and tensile strength of 28 and 1.6 MPa, respectively, sustaining up to 800% stretches.[27] The carbonyl group of DMAA and the carboxylic acid group of MAAc acting as the H-bond acceptor and donor, respectively, create multiple H-bonds between the copolymer chains, leading to the formation of polymer-rich aggregates stabilized by the hydrophobic α-methyl groups of MAAc units. These aggregates sacrificially rupture under stress by dissipating energy while the ductile polymer-poor region maintains the hydrogel integrity.[27] Recently, it has been shown that the free-radical polymerization of MAAc in aqueous solutions without DMAA also produces mechanically strong hydrogels when *N*,*N*,*N*′,*N*′-tetramethylethylenediamine (TEMED), a popular accelerator, was included into the reaction system.[30] The cooperative H-bonds between MAAc and TEMED leads to a microphase separation and hence formation of a sponge-like hydrogel.

UV polymerization of 2-acrylamido-2-methyl-1-propanesulfonic acid (AMPS) and DMAA in aqueous solutions at a water content of 40 wt % produces H-bonded superabsorbent hydrogels that are stable in water and absorb 1000 times their weight in water.[31] It was shown that both the strong H-bonding interactions between AMPS and DMAA units and multiple H-bonds between the polymer chains due to the proximity effect are responsible for the integrity of the hydrogels even at high swelling ratios.

Copolymerization of methacrylamide (MAAm) and MAAc in aqueous solutions at a water content of 50−60 wt % produces tough and stiff hydrogels at 15−35 mol % MAAm due to multiple H-bonding between amide and carboxylic acid groups inducing a microphase separation.[32] Wu and co-workers reported that the copolymers of 1-vinylimidazole (NVI) and acrylic acid (AAc) at a water content between 35 and 50 wt % are tough physical hydrogels due to the H-bonds between imidazole and carboxylic acid groups.[33] They exhibit a tensile stress and Young's modulus of up to 1.8 and 0.7 MPa, respectively. Replacing AAc with the MAAc monomer and in the presence of 50−60 wt % water, the tensile stress and modulus of these hydrogels further increase up to 5.4 and 170 MPa, respectively.[28] Due et al. investigated the mechanical properties of H-bonded hydrogels based on acrylamide (AAm) and MAAc with 50−60 wt % water by focusing the role of H-bonds at different timescales.[34] Physical hydrogels with the highest toughness and good water stability were obtained at 20−35 mol % AAm, which is attributed to the dense H-bonds between the monomer units.

In summary, a large number of works have been done in recent years for preparing copolymer hydrogels using different monomers under various experimental conditions such as the water loading at the gel preparation affecting significantly the hydrogel properties.[34] In light of the diversity of the gelation conditions, there exists no clear evidence how the competing intermolecular interactions determine formation of mechanically robust physical hydrogels. The aim of this study was to prepare a series of copolymer hydrogels by combining different monomeric units bearing H-bond donor and acceptor atoms. The gel formation was achieved under identical conditions by changing the type and the molar ratio of the comonomers to elucidate the impact of H-bonding on the physical cross-linking ability of the polymer chains. We selected the following monomers that are widely used in the preparation of hydrogels: methacrylic acid (MAAc), acrylic acid (AAc), *N*,*N*-dimethylacrylamide (DMAA), 1-vinylimidazole (NVI), *N*-vinyl pyrrolidone (NVP), and acrylamide (AAm). Figure 1A shows the chemical structure of the monomer units which constitute the copolymers and the electrostatic potential (ESP) charges on their H-bond donor and acceptor atoms. The optimized geometries of those monomers in water reveal the formation of strong H-bonds between sterically unhindered carbon oxygen or pyridinic nitrogen atoms of the monomers and water with energies between 6 and 8 kcal·mol^{-1} (Table S1). Because such strong monomer−water interactions weaken the inter-chain H-bonds and hence the mechanical strength of the resulting H-bonded hydrogels, a hydrophobic microenvironment in the hydrogel network seems to be an important factor to increase the inter-chain H-bond density.[35] The hydrophobicity of the selected monomers was quantified

https://doi.org/10.1021/acs.macromol.2c01469
Macromolecules 2022, 55, 10576−10589

Table 1. Mechanical Parameters of Four Sets of Copolymer Hydrogels[a]

Set	M_1	M_2	n_1/n_2	E/MPa	σ_f/MPa	W/MJ· m^{-3}	ε_f %
1	MAAc	DMAA	4/1	2.8 (0.1)	3.3 (0.2)	15 (1.7)	650 (56)
	AAc	DMAA	4/1	0.16 (0)	0.16 (0)	3.9 (0.4)	3200 (240)
2	AAc	DMAA	4/1	0.16 (0)	0.16 (0)	3.9 (0.4)	3200 (240)
	AAc	NVI	4/1	0.55 (0.05)	1.8 (0.2)	4.7 (0.4)	550 (37)
3	AAc	NVI	9/1	0.27 (0.01)	0.29 (0.02)	1.5 (0.2)	650 (50)
	MAAc	NVI	9/1	18.7 (0.8)	3.3 (0.1)	11.4 (0.8)	290 (30)
4	AAm	NVP	6/1	0.20 (0.05)	0.20 (0.02)	2.1 (0.3)	1400 (50)
	MAAc	NVP	6/1	0.95 (0.07)	1.02 (0.09)	3.2 (0.6)	400 (60)

[a]The molar ratio n_1/n_2 of the comonomers M_1 and M_2 corresponds to the critical comonomer composition at which a maximum in the mechanical strength and stiffness is observed. Standard deviations are in parentheses. E = Young's modulus. σ_f and ε_f = fracture stress and strain, respectively. W = toughness (energy to break).

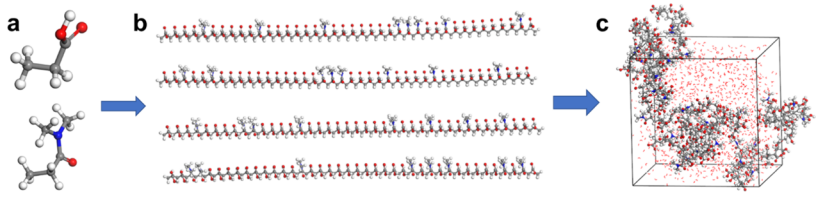

Figure 2. Modeling steps for the construction of cells for AAc/DMAA at a mole ratio of 4/1. (a) Molecular structures of AAc and DMAA. (b) Four different random copolymers each composed of 40 monomers. (c) Amorphous cell generated for MD simulations containing 60 wt % water. The simulation box shows the snapshot picture of equilibrium structure of the AAc_{32}-$DMAA_8$ random copolymer at 298 K.

by the octanol−water partition coefficient log P. The monomers with a positive log P prefer to partition into the 1-octanol layer and hence exhibit hydrophobic character, while those with a negative log P are hydrophilic and dissolve in the water layer. Here, we compare the hydrophobicity of the monomers using solvent-accessible SA-normalized log P values (log P/SA), which predict well the extent of interactions between thermosensitive copolymers in water.[35] Figure 1B and Table S2 presenting the log P/SA values of the monomers and pentamers reveal that the hydrophobicity significantly changes depending on the type of the monomers.

The copolymer hydrogels based on MAAc/DMAA, AAc/DMAA, AAc/NVI, MAAc/NVI, MAAc/NVP, and AAm/NVP were prepared at various molar ratios in the presence of 60 wt % water, and their mechanical parameters were determined at a fixed experimental timescale. As will be seen below, most of the resulting H-bonded hydrogels are stable in water, but they all dissolve in aqueous urea or alkaline solutions and exhibit a maximum in the mechanical strength at a critical comonomer composition. The Young's modulus of the hydrogels varies between 10^{-1} and 10^{1} MPa that can be tuned by the type and composition of the comonomer mixture. The hydrophobicity of the monomers and the competing interactions between the copolymer chains and copolymer−water were quantitatively elucidated by the all-atom molecular dynamics (MD) simulations in the explicit water, density functional theory (DFT) calculations, and molecular descriptors by remaining faithful to the experimental compositions. As will be seen below, the main factors determining the mechanical performance of the copolymer hydrogels are the hydrophobicity of the major copolymer component, formation of ionic H-bonds, appearance of strong H-bonded nanoaggregates during polymerization, and stronger and higher inter-chain H-bonding and hence electrostatic interactions.

EXPERIMENTAL PART

Hydrogel Synthesis and Characterization. All the copolymerization reactions were conducted in distilled water in the presence of an Irgacure 2959 photoinitiator at 23 ± 2 °C under UV light at 360 nm for 24 h. The water content of the hydrogels was kept at 60 wt %, which is similar to soft tissues and load bearing tissues such as ligaments, tendons, and cartilages.[36] The copolymer hydrogels synthesized by combining the monomers at different molar ratios were MAAc/DMAA, AAc/DMAA, AAc/NVI, MAAc/NVI, MAAc/NVP, and AAm/NVP. Typically, to prepare MAAc/DMAA copolymer hydrogels with 20 mol % DMAA (molar ratio 4/1), MAAc (3.10 g) and DMAA (0.90 g) were dissolved in 6.0 g of water at room temperature. After dissolving Irgacure 2959 (20.3 mg), the solution was transferred into several 1 mL plastic syringes of 4.6 mm internal diameter, and the polymerization reactions were conducted in a UV reactor at 23 ± 2 °C for 24 h under UV light.

The uniaxial tensile tests were conducted on hydrogel specimens of 4.6 mm diameter and 60 mm length. The tests were performed at 23 ± 2 °C on a Zwick Roell Z0.5 TH test machine using a 500 N load cell. The initial sample length between the jaws was fixed at 10.0 ± 0.1 mm. The tests were conducted at a constant crosshead speed of 10 and 50 mm min^{-1} below and above 15% strain, respectively. From the load and displacement data, the nominal stress σ_{nom}, which is the force per cross-sectional area of the undeformed gel specimen, and strain ε (deformed length/original length) were calculated. Young's modulus E of the hydrogels was calculated from the slope of the stress−strain curves between 5 and 15% strain. The energy to break W (toughness) was calculated from the area under the stress−strain curves up to the fracture point. The mechanical parameters of the hydrogels at the critical compositions are compiled in Table 1. Cyclic tensile tests were conducted at a fixed crosshead speed of 50 mm min^{-1} up to a maximum strain of 250%. All copolymer hydrogels were subjected to five successive tensile cycles with a waiting time of 1 min between cycles. The details of the hydrogel preparation, solubilization tests in aqueous urea and alkaline solutions, and their characterizations are given in the Supporting Information.

Computational Methods. The ESP charges on H-bond donor and acceptor atoms of the monomer units were calculated by the DFT method at the B3LYP/6-31g (d,p) level (Figure 1A). Pairwise interactions between the monomers and water were calculated at the M06-2X/6-31g(d,p) level. Different types of random copolymers were

https://doi.org/10.1021/acs.macromol.2c01469
Macromolecules 2022, 55, 10576−10589

Table 2. Summary of E_{elec} and E_{vdW} Energies and Their Fractions with Respect to the Total and Non-bonded (nonb) Energies per Atom (kcal·mol^{-1}) for the Studied Copolymer Systems in Water Calculated by MD Simulations

Set	M_1	M_2	n_1/n_2	E_{elec}	E_{vdW}	E_{vdW}/E_{total}	E_{elec}/E_{total}	E_{elec}/E_{nonb}
1	MAAc	DMAA	4/1	−2.84	0.56	−0.38	1.93	1.24
	AAc	DMAA	4/1	−3.24	0.51	−0.25	1.59	1.19
2	AAc	DMAA	4/1	−3.24	0.51	−0.25	1.59	1.19
	AAc	NVI	4/1	−3.34	0.49	−0.22	1.52	1.17
3	AAc	NVI	9/1	−3.45	0.51	−0.22	1.51	1.11
	MAAc	NVI	9/1	−2.96	0.56	−0.35	1.86	1.23
4	AAm	NVP	6/1	−3.76	0.41	−0.14	1.29	1.12
	MAAc	NVP	6/1	−3.01	0.53	−0.31	1.79	1.21

built by using six different monomers, namely, MAAc, AAm, AAc, DMAA, NVP, and NVI. Copolymer hydrogels based on MAAc/DMAA (4/1), AAc/DMAA (4/1), MAAc/NVP (4/1 and 6/1), AAc/NVI (4/1 and 9/1), MAAc/NVI (4/1 and 9/1), and AAm/NVP (6/1) were modeled at critical molar ratios (as given in parenthesis) using Materials Studio Visualizer.[37] In addition to the nonionic NVI, AAc, and MAAc monomers, their ionic forms were also modeled by randomly generating equal numbers of NVI^+ and AAc^- or $MAAc^-$ along the chain.[38] Each chain was composed of 40 monomers having different random monomer distributions along the chain as given in Figure 2 for AAc/DMAA at a mole ratio of 4/1. Amorphous cells with a density of 1.00 g·mL^{-1} were constructed by using four random copolymer chains having 60 wt % water.

For each copolymer, 20 different amorphous cells were constructed. Molecular mechanics (MM) minimizations were performed for 5000 steps, and the amorphous cells with lowest energies were subjected to molecular dynamics (MD) simulations. MD simulations (2 ns) with a time step of 1fs were performed at the NVT ensemble using a Nose Thermostat at 298 K. Compass force field (CFF) present in the Discover module of Materials Studio software was used in all calculations.[39,40] Frame output for atomic coordinates and energies were saved in the last 500 ps of simulations at every 5000 steps. The post MD analyses of potential energy components and radial distribution functions were conducted to explore the competing interactions between polymer chains and water molecules. The experimental findings were supported at the molecular level by the calculations of electrostatic and van der Waals (vdW) energies of the copolymers in water, monomer−monomer and monomer−water mixing energies,[41] and free energy of solvation.[42] The details of the calculations are given in the Supplementary Information section and Tables S3 and S4. A QSAR hydrophobicity descriptor calculation for atom-type-based log P was also performed,[43] which was normalized by solvent-accessible SA of the repeating units (log P/SA),[44] that was recently demonstrated to present as a successful method to compare hydrophilic/hydrophobic balance of the copolymers.[35] Tables 2 and 3 summarize the electrostatic (E_{elec}) and van der Waals (E_{vdW}) energies per atom of the copolymers in water, monomer−monomer, and monomer−water mixing energies (E^{ij}_{mix}).

RESULTS AND DISCUSSION

The copolymerization reactions of six different comonomer pairs in aqueous solutions at a water content of 60 wt % were conducted under identical conditions. The physical hydrogels obtained after a reaction time of 24 h exhibited a wide range of mechanical parameters, namely, Young's modulus E, fracture stress σ_f and strain ε_f, and toughness W (energy to break), at a fixed experimental timescale, depending on the type and composition of the comonomers (Table 1). In the following sections, we compare the mechanical properties of the copolymer hydrogels by fixing one of the monomer type while changing the second one. Thus, four sets of comparisons were made: (i) MAAc/DMAA versus AAc/DMAA, (ii) AAc/DMAA versus AAc/NVI, (iii) AAc/NVI versus MAAc/NVI, and (iv) AAm/NVP versus MAAc/NVP. The competing H-bonding interactions between copolymer−copolymer and copolymer−water were studied quantitatively by DFT calculations and MD simulations. The interplay of various factors on the H-bond density and the roadmap in designing mechanically robust copolymer hydrogels are presented in the last two sections.

Table 3. Calculated Monomer−Monomer and Water−Monomer Mixing Energies E^{ij}_{mix} (in kcal·mol^{-1}) at 298 K

i	j	E^{ij}_{mix}
MAAc	NVI	−0.31
MAAc	DMAA	−0.36
AAc	NVI	−0.46
AAc	DMAA	−0.49
MAAc	NVP	−2.15
AAm	NVP	−2.75
water	MAAc	1.61
water	AAc	1.56
water	AAm	−0.28
water	DMAA	−2.09
water	NVI	−3.25
water	NVP	−6.04

MAAc/DMAA versus AAc/DMAA. To highlight the effect of the hydrophobic α-methyl group on the mechanical properties of the physical copolymer hydrogels, we first compare MAAc/DMAA and AAc/DMAA hydrogels with various amounts of DMAA between 0 and 100 mol %. Figure 3a,b shows their stress−strain curves where the red curves represent the data of the corresponding homopolymer hydrogels, namely, PMAAc, PAAc, and PDMAA. The insets are the zoom-in representation of the data at below 1350% strain (a) and 0.2 MPa stress (b). Figure 3a reveals that the DMAA component alone (denoted by "100" in the figure) produces a highly stretchable homopolymer hydrogel sustaining to 5500% stretch ratio with a low Young's modulus E (43 ± 6 kPa), while MAAc alone (denoted by "0") forms a brittle homopolymer hydrogel with a stretch ratio at a break of 306 ± 8% but around 8 times higher modulus (334 ± 7 kPa). The incorporation of DMAA units into the brittle PMAAc hydrogel network drastically increases the mechanical parameters until attaining a maximum value at 20 mol % DMAA, as can be seen in Figure 4. At this composition, the hydrogel exhibits the highest Young's modulus E (2.8 ± 0.1 MPa), fracture stress σ_f (3.3 ± 0.3 MPa), and toughness W (15 ± 1.7 MJ·m^{-3}).

In contrast to the brittle PMAAc hydrogel, PAAc forms a highly stretchable (2800%) and tough hydrogel (2.8 vs 0.3 MJ·m^{-3}) (Figures 3b and S1). Replacing the MAAc component of the copolymer with AAc results in a mechanically weak

https://doi.org/10.1021/acs.macromol.2c01469
Macromolecules 2022, 55, 10576−10589

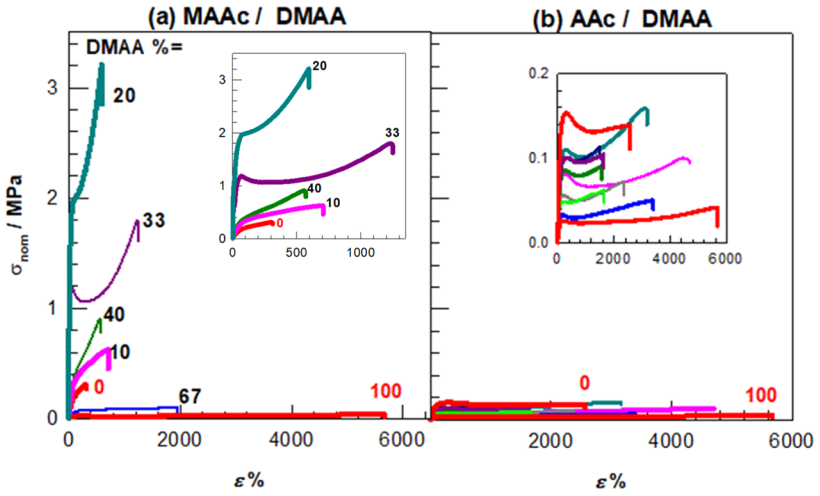

Figure 3. Stress−strain curves of MAAc/DMAA (a) and AAc/DMAA hydrogels (b) at various compositions. In (b), DMAA contents are 10 (pink), 20 (dark cyan), 25 (dark blue), 33 (dark pink), 40 (dark green), 50 (dark gray), 60 (green), and 67 mol % (blue). The insets are the zoom-in representation of the data at below 1350% strain (a) and 0.2 MPa stress (b).

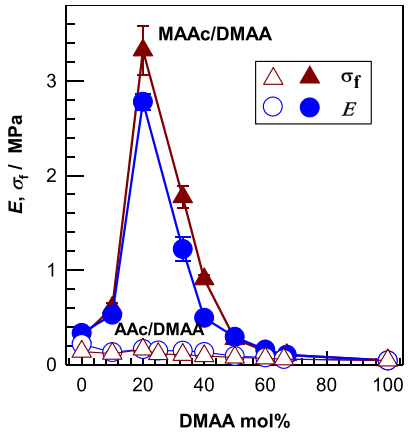

Figure 4. Young's modulus E and the fracture stress σ_f of MAAc/DMAA (filled symbols) and AAc/DMAA hydrogels (open symbols) plotted against DMAA mol %.

hydrogel over the whole range of DMAA content (Figures 3b, 4). The stress−strain curves for AAc/DMAA hydrogels remain between those of the PAAc and PDMAA hydrogels, and their modulus and strength do not change with the comonomer composition. The MAAc/DMAA hydrogel with 20 wt % DMAA exhibits 18- and 21-fold higher E and σ_f, respectively, as compared to the AAc/DMAA hydrogel highlighting the importance of the hydrophobic α-methyl group on MAAc units.

Cyclic mechanical tests that are conducted up to a strain below the fracture point are a mean to determine the extent of energy dissipation in hydrogels. In the case of H-bonded hydrogels, microscopic damage due to the breaking of H-bonds under strain is evidenced by the magnitude of the area enveloped by the loading and unloading curves, which is denoted as the hysteresis energy U_{hys}. We conducted five successive cyclic tensile tests with a time interval of 1 min by stretching MAAc/DMAA and AAc/DMAA hydrogels up to a maximum strain of 250%, followed by unloading to zero strain. Figure 5 shows these cycles for MAAc/DMAA (a) and AAc/DMAA hydrogels (b). For both hydrogels, the first mechanical cycle shows a slightly higher hysteresis area, while the following cycles are close to reversible revealing dissociation and reformation of the H-bonds. Moreover, although a residual strain appears after each unloading, the initial length of the test specimens is recovered during the waiting time between the cycles. Figure 6a,b presents the U_{hys} of MAAc/DMAA and AAc/DMAA hydrogels, respectively, with various DMAA contents plotted against the cycle number. For MAAc/DMAA hydrogels, U_{hys} increases by an order of magnitude with increasing amount of DMAA up to 20 mol % DMAA, as indicated by an arrow in the figure, and then again decreases to a low value. This indicates that the hydrogel with 20 mol % DMAA has the largest number of inter-chain H-bonds, as can be expected from its high cross-link density represented by the modulus E (Figure 4). In contrast, the U_{hys} of AAc/DMAA hydrogels is very low, and it further decreases as the DMAA content is increased, signifying the existence of fewer and weaker H-bonds (Figure 6b).

We attribute the higher mechanical properties of MAAc/DMAA hydrogels as compared to the AAc/DMAA ones to the significant energy dissipation of the former hydrogels due to the sacrificial bonds breaking under strain. This can also be evidenced in stress−strain curves showing a clear yielding point, followed by necking behavior, which significantly increases the mechanical properties (Figure 3). This also suggests the existence of strong and weak H-bonded regions in the hydrogel, resembling the first and second networks of the double-network hydrogels.[2] Thus, strong H-bonded regions break into fragments at the yield point, while the weak H-bonded regions maintain the macroscopic sample together, leading to toughness improvement. The yielding in MAAc/DMAA hydrogels starts to appear at 20 mol % DMAA with a yield stress of 2 MPa, while increasing DMAA content decreases the yield stress and finally disappears at 40 mol % DMAA (Figure 3a). Although the yielding behavior also appears for AAc/DMAA hydrogels (inset to Figure 3b), the yield stress is 1 order of magnitude lower than the former hydrogels, revealing the existence of weaker H-bonds producing lesser amount of energy dissipation.

Higher modulus (18-fold) of MAAc/DMAA hydrogel as compared to AAc/DMAA at 20 mol % DMAA was also reflected in their swelling behavior in water. Although the swelling ratio m_{rel} of AAc/DMAA hydrogel is 4350 ± 200 after 20 days, and it gradually disintegrates at longer times, m_{rel} of

https://doi.org/10.1021/acs.macromol.2c01469
Macromolecules 2022, 55, 10576−10589

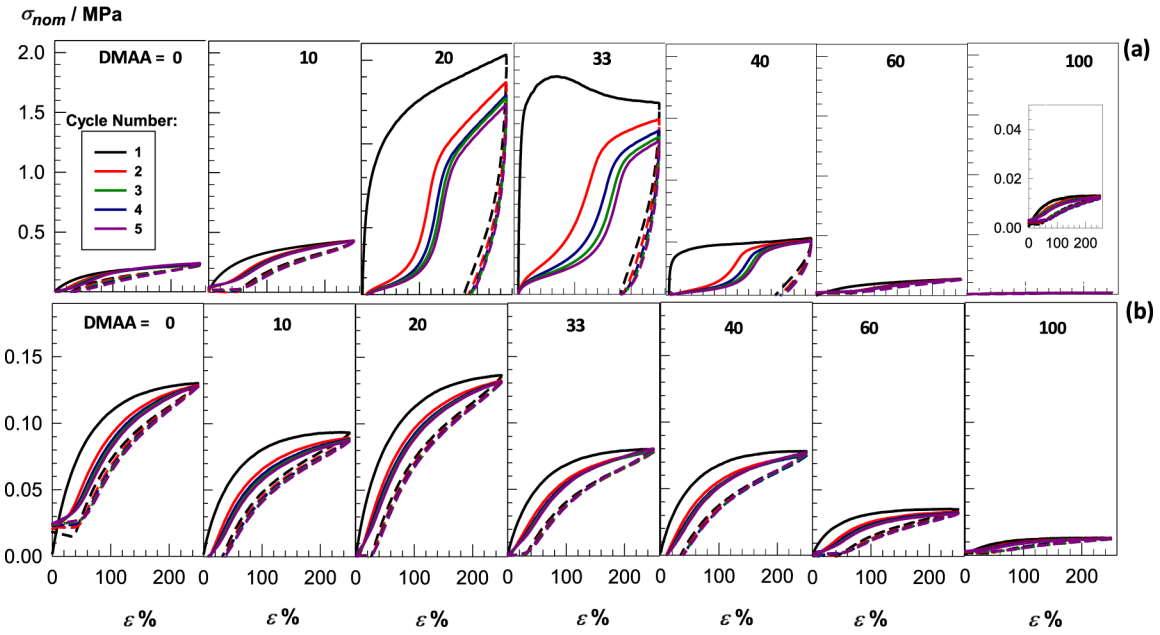

Figure 5. Five successive loading−unloading cycles for MAAc/DMAA (a) and AAc/DMAA hydrogels at various compositions as indicated. The solid and dashed lines show the loading and unloading curves, respectively.

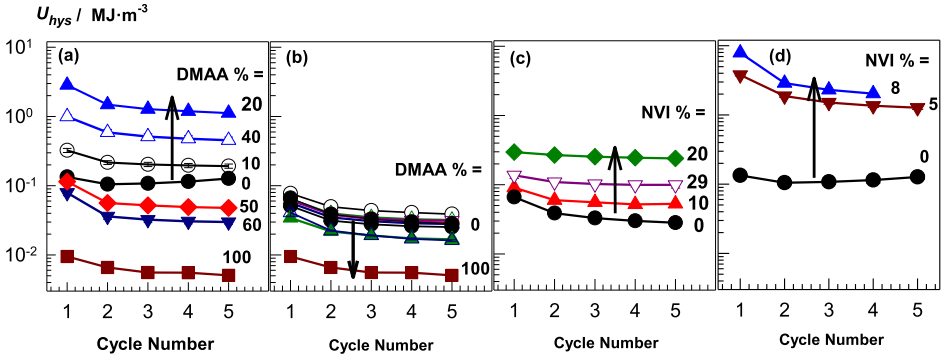

Figure 6. Hysteresis energies U_{hys} of MAAc/DMAA (a), AAc/DMAA (b), AAc/NVI (c), and MAAc/NVI hydrogels (d) at various compositions plotted against the cycle number. In (b), the explanation of the symbols is the same as given in (a).

MAAc/DMAA remains at around unity (1.0 ± 0.1) over 1 month. One may argue that because of the self-cross-linking ability of DMAA monomer,[27] its polymerization in aqueous solutions without a chemical cross-linker may lead to the formation of chemical cross-linked hydrogels. However, MAAc/DMAA hydrogel with 20 mol % DMAA could easily be dissolved in an aqueous solution of 7 M urea, a H-bond breaking agent, within 2 weeks at 23 ± 2 °C to form a homogeneous polymer solution. A similar result was also obtained with the AAc/DMAA hydrogel reflecting the physical nature of both hydrogels.

The results thus reveal the formation of mechanically strong and tough physical hydrogels via H-bonds when MAAc instead of AAc is used as a comonomer of DMAA. To explain this finding and also to emphasize the impact of the hydrophobic α-methyl group on the mechanical properties of the physical hydrogels, we first compare the calculated hydrophobicity of the monomers in terms of the normalized octanol−water partition coefficient log P/SA (Figure 1B and Table 2). MAAc is more hydrophobic than AAc, and its interaction with water is less than that of AAc (Table 3). Because the strength of the H-bonds increases with increasing hydrophobicity in the microenvironment of H-bond forming groups,[27,45,46] log P/SA coefficients reveal that the physical cross-link density of MAAc/DMAA hydrogel would be higher than that of the AAc/DMAA one.

This behavior was also captured in the radial distribution functions (RDFs) of polymer−water and polymer−polymer interactions. The calculated carboxylic acid hydrogen (H_{COOH})—water oxygen ($H_{COOH}\cdots O_w$) RDFs display an average H-bond distance of around 1.9 Å (Figure S2). Although the average H-bond distance is more or less the same for both MAAc/DMAA and AAc/DMAA hydrogels, the maxima of the RDF peaks for polymer−water interactions are more intense for the less hydrophobic AAc/DMAA hydrogel (Figures 7a and S2). Figure 7b showing the RDFs of polymer−polymer interactions between the carbonyl oxygen of carboxylic acid (O_{COOH}) and H_{COOH} also reveals that the AAc units form a higher amount of inter-chain H-bonding between carboxylic acid units. However, its dominant H-bonding interaction is mainly with the water molecules that reduce the mechanical properties. The higher number of interactions with water in AAc/DMAA hydrogel is also reflected in the calculated electrostatic energies (E_{elec}) per

https://doi.org/10.1021/acs.macromol.2c01469
Macromolecules 2022, 55, 10576−10589

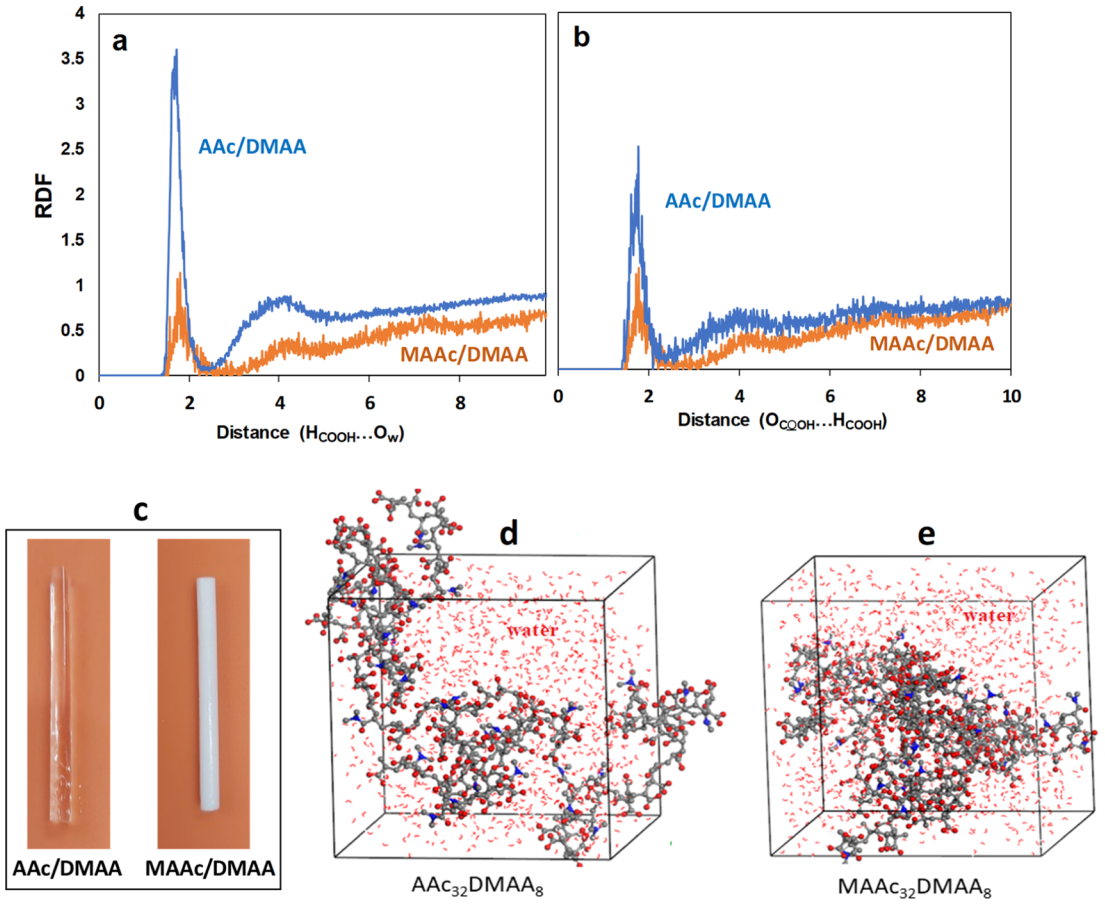

Figure 7. (a,b) Radial distribution function of polymer−water (a) and polymer−polymer (b) interactions in MAAc/DMAA and AAc/DMAA hydrogels by MD trajectory analysis. (c) Optical images of AAc/DMAA and MAAc/DMAA hydrogels formed at 20 mol % DMAA. (d,e) Snapshot pictures of equilibrium structures of four $AAc_{32}/DMAA_8$ (d) and $MAAc_{32}/DMAA_8$ copolymer chains (e) composed of 40 monomer units in 60 wt % water obtained by MD simulations.

atom, which increases (becomes more negative) as a result of increased H-bonding interactions (Table 2). Moreover, the higher vdW interactions of MAAc are attributed to the presence of the α-methyl group which AAc does not have.

Thus, the higher log P and lower E_{elec} per atom values of MAAc/DMAA are an indication of its enhanced physical cross-linking density when compared to that of AAc/DMAA hydrogel. Another parameter affecting the number of H-bonds and also favoring the development of the microphase separated domains is the competition of the effective (H-bond forming) interactions between monomer−monomer and monomer−water pairs. The calculated mixing energies, E^{ij}_{mix}, given in Table 3 simply attest the winner of this competition. The mixing energy of MAAc with DMAA is less negative and that with water is more positive than those of AAc predicting the phase separation tendency of MAAc/DMAA copolymer from water. Indeed, in contrast to the transparent AAc/DMAA hydrogels, opaque MAAc/DMAA hydrogels were obtained at 20 mol % DMAA (Figure 7c). The calculated energies are also consistent with the hydrophobicity differences between the segments of the copolymers and indicate the segregation of MAAc units along the copolymer chains facilitating cooperative inter-chain H-bonding between MAAc and DMAA units. Snapshot pictures of equilibrium structures of four $AAc_{32}/DMAA_8$ and $MAAc_{32}/DMAA_8$ copolymer chains composed of 40 monomer units in 60 wt % water obtained by MD simulations shown in Figure 7d,e also reveal their diluted and aggregated configurations, respectively. Lower water mixing energy of MAAc units enhances the inter-chain H-bond formation due to the exclusion of water from the copolymer nanoenvironment.

AAc/DMAA versus AAc/NVI and MAAc/NVI. The second set of the comonomer pairs contains imidazole and carboxylic acid functional groups, which are typical H-bond donor and acceptor pairs, respectively, forming robust H-bonds in aqueous media.[28,33,38,47] Indeed, we observed that the mechanically weak AAc/DMAA copolymer hydrogel detailed above turns into a strong hydrogel when its DMAA units are replaced with the NVI ones. Figure 8a shows the stress−strain curves of AAc/NVI hydrogels at various NVI contents, while Figure 8b shows the comparison of their modulus E and fracture stress σ_f with those of the AAc/DMAA ones. Both E and σ_f of AAc/NVI hydrogel increase with increasing amount of NVI until attaining maximum values at 20 mol %, that is, 0.55 ± 0.05 and 1.8 ± 0.2 MPa, respectively, at which it sustains 550 ± 40% elongation. This trend and values are consistent with those of AAc/NVI hydrogels prepared in DMSO, followed by solvent exchange to water.[33] The formation of additional H-bonds by replacing DMAA with NVI is also reflected by the increasing extent of energy dissipation under strain, as estimated from cyclic mechanical tests (Figure S3). In contrast to AAc/DMAA hydrogels, the U_{hys} of AAc/NVI hydrogel increases with increasing amount of NVI up to 20 mol % and then decreases again (Figure 6b,c).

https://doi.org/10.1021/acs.macromol.2c01469
Macromolecules 2022, 55, 10576−10589

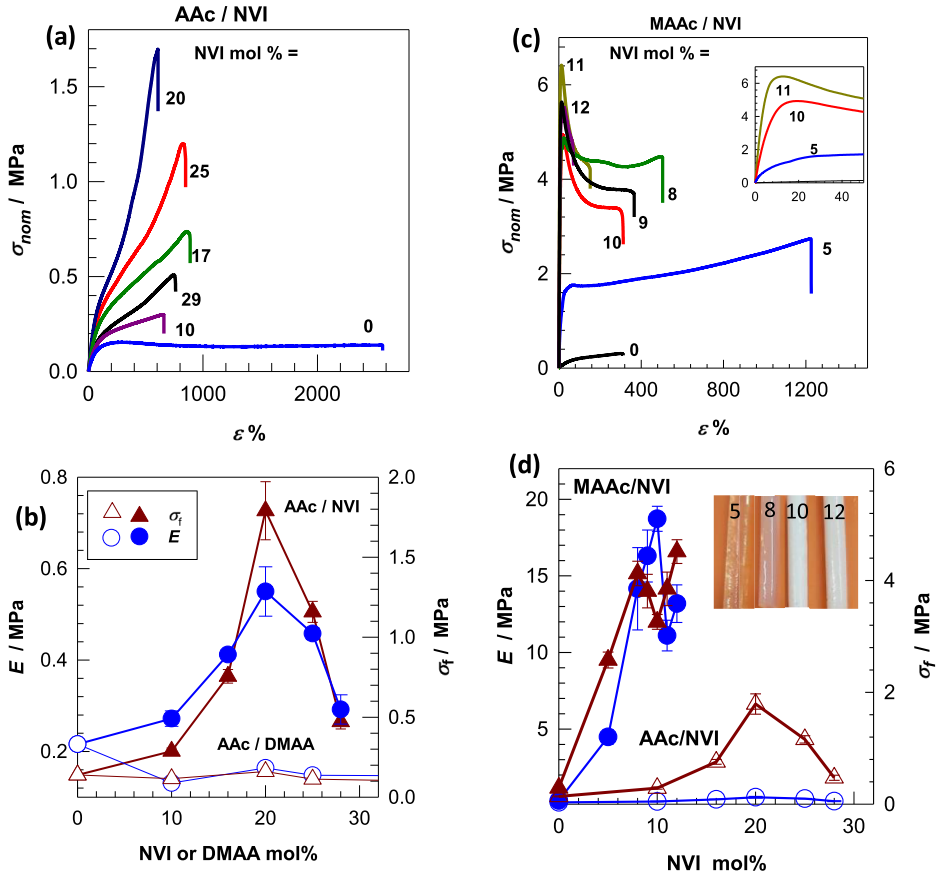

Figure 8. (a,b) Stress−strain curves (a) and mechanical parameters (b) of AAc/NVI hydrogels at various compositions. For comparison, the mechanical data of AAc/DMAA hydrogels are shown in (b) by the open symbols. (c) Stress−strain curves of MAAc/NVI hydrogels at various compositions. The inset shows the same curves for hydrogels with 5, 10, and 11 mol % NVI up to 50% strain. (d) Mechanical parameters of MAAc/NVI hydrogels plotted against NVI mol %. For comparison, the mechanical data of AAc/NVI hydrogels are shown by the open symbols. The symbols have the same meaning as in Figure 9b. The inset shows the images of MAAc/NVI hydrogel specimens prepared at various mol % NVI as indicated.

The mechanical properties of AAc/NVI hydrogels could be further increased when AAc units are replaced with the MAAc ones (Figure 8c,d). In contrast to the former hydrogels, MAAc/NVI hydrogels exhibit a significant yielding behavior at 10−20% strain with a yield stress increasing with the NVI content up to 11 ± 1 mol % (inset to Figure 8c). The maximum in E and σ_f observed at 20 mol % NVI for AAc/NVI hydrogels shifts to 10 mol % NVI by replacing AAc with MAAc, at which the hydrogel exhibits a modulus of 18.7 ± 0.8 MPa, which is the highest value obtained from all comonomer pairs. Visual observation showed that the transparent MAAc/NVI hydrogel at 5 mol % NVI becomes hazy at 8 mol % and finally turns into opaque at and above 10 mol % (images in Figure 8d). This indicates NVI-induced phase separation, leading to the coexistence of highly and loosely cross-linked regions in MAAc/NVI hydrogels, as similar to the MAAc/DMAA ones (Figure 7c). Some scatter in the mechanical data at around 10 mol % NVI is thus attributed to the heterogeneity of the gel samples (Figure 8d).

Cyclic mechanical tests up to a maximum strain of 250% were also conducted on MAAc/NVI hydrogels at various DMAA contents (Figure S4). At or above 10 mol % NVI, the hydrogel specimens macroscopically fractured during the second mechanical cycle, while at 8 mol % NVI, the tests without a macroscopic failure could be conducted up to the fourth cycle. It is likely that the propagation rate of internal cracks in these hydrogels is too fast, and the energy dissipation mechanism does not prevent crack propagation due to their heterogeneous structure. The hysteresis energies U_{hys} of the hydrogels with 0−8 mol % NVI shown in Figure 6d indicate a significant higher hysteresis as compared to AAc/NVI hydrogels reflecting the existence of a higher number and/or stronger H-bonds in the physical MAAc/NVI network. Both AAc/NVI and MAAc/NVI hydrogels with 20 and 10 mol % NVI, respectively, that is, at their critical comonomer compositions, were insoluble in water with a weight swelling ratio m_{rel} of around unity (1.00 ± 0.15 and 1.00 ± 0.04, respectively). Although AAc/NVI hydrogel could be dissolved in aqueous 7 M urea solution, MAAc/NVI hydrogel was insoluble in this solution after 3 months and preserved its shape.

All these features of NVI-containing copolymer hydrogels reflect the existence of strong H-bonds between NVI and AAc or MAAc segments. However, considering the log P/SA values (Figure 1B and Table S1), NVI is more hydrophilic than AAc with a good single-proton acceptor through its pyridinic nitrogen atom of the imidazole ring. Indeed, it prefers to form much stronger H-bonds with water than with MAAc and AAc units, as reflected in water mixing energies (Table 3). The snapshot pictures of equilibrium structures of $MAAc_9NVI_1$, $MAAc_4NVI_1$, and AAc_4NVI_1 copolymers from MD simulations also reveal a transition from aggregated-to-diluted config-

https://doi.org/10.1021/acs.macromol.2c01469
Macromolecules 2022, 55, 10576−10589

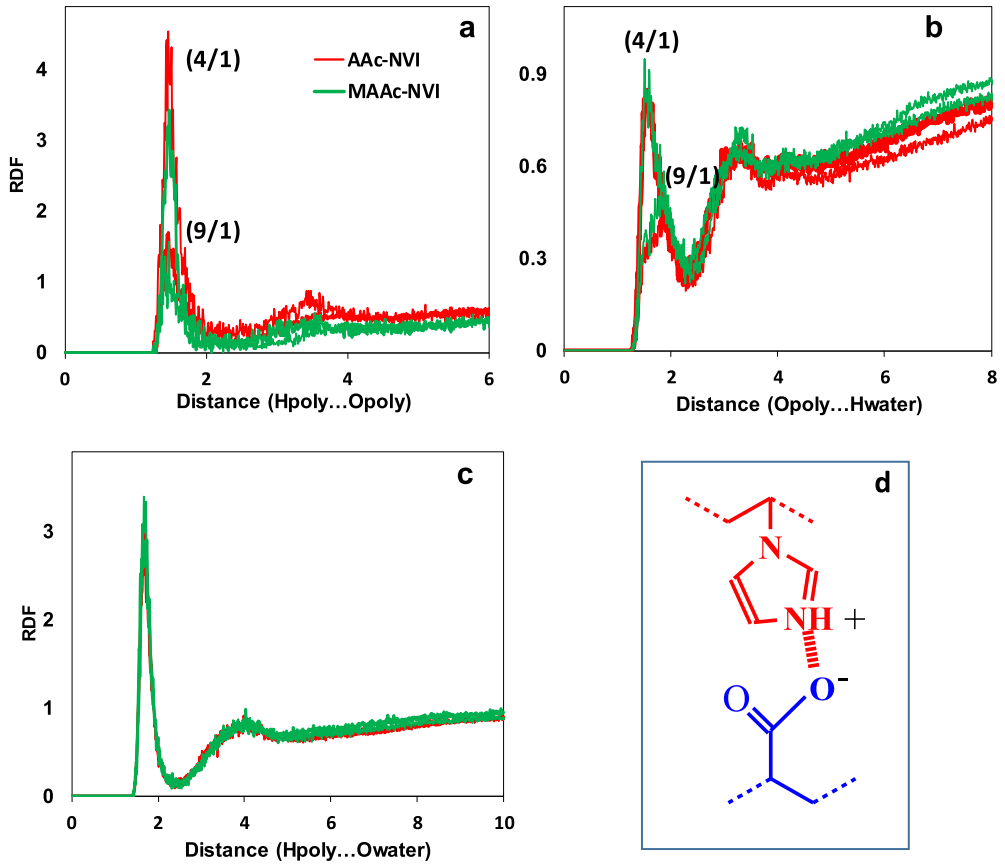

Figure 9. (a–c) RDFs of polymer–polymer (a) and polymer–water interactions (b,c) for AAc/NVI (red) and MAAc/NVI hydrogels (green). The molar ratio of the comonomers is indicated. H_{poly} and O_{poly} means H-bond forming hydrogens and oxygens in the copolymers, respectively. (d) Chemical structure of imidazolium–carboxylic acid salt formed via the ionic H-bond.

uration of the copolymer chains in water as the NVI content is increased, or MAAc units are replaced with the AAc ones at a fixed NVI content (Table S5). The comparison of RDFs of AAc/DMAA and AAc/NVI hydrogels at a comonomer ratio of 4/1 reveals that AAc/NVI forms a higher number of H-bonding both with water and other chains (Figure S5). Figure 9a–c shows the RDFs of polymer–polymer (a) and polymer–water interactions of AAc/NVI and MAAc/NVI hydrogels at two different comonomer ratios as indicated. Both hydrogels form a comparable amount of polymer–polymer and polymer–water interactions via H-bonds at the same comonomer ratio.

The simulation results thus indicate that the NVI-containing hydrogels and the AAc/DMAA ones exhibit comparable H-bonding interactions and hence unable to explain the high modulus approaching to 20 MPa for the MAAc/NVI system (Table 1). We should note that our calculations assume a fixed chemical structure in the classical simulations for the polymer segments. However, the imidazole groups alone or pendant to hydrophilic polymer chains are known to deprotonate carboxylic acid groups to form imidazolium carboxylate salts via ionic H-bonds (Figure 9d).[38,47,48] The ionic H-bonds interconnecting the copolymer chains are much stronger than the H-bonds between neutral molecules, which may significantly contribute to the stiffness of the hydrogels. Indeed, the solubility measurements revealed that although MAAc/NVI hydrogels are insoluble in water or in aqueous 7 M urea, they could easily be dissolved in aqueous strong alkaline (pH > 11) solutions revealing dissociation of ionic H-bonds. MD simulations were also performed by protonation of all NVI repeat units (NVI^+) in the copolymer chains and deprotonation of equal number of AAc or MAAc repeat units (AAc^- and $MAAc^-$). Calculations showed stronger electrostatic interactions between ionic comonomers than the neutral ones, revealing enhanced hydrogen bonding (Table S6). Simultaneously, a 3 orders of magnitude increase in the mixing energy between imidazolium cations (NVI^+) and carboxylate anions ($MAAc^-$ and AAc^-) was observed as compared to the neutral NVI and AAc or MAAc (Table S7). This would lead to the aggregations and phase separation of imidazolium salt-rich domains in the hydrogels with limited amount of water adsorption. The dramatic increase in the mechanical properties of the hydrogels in any composition upon replacing AAc with MAAc can thus be attributed to the formation of cooperative ionic H-bonds accompanied by microphase separation. Thus, multiple ionic H-bonds between NVI and MAAc units lead to the formation of less-swollen aggregates in hydrogels that are stabilized by α-methyl groups of MAAc. The microscopic rupture of the aggregates under strain leads to energy dissipation while the swollen region of the hydrogel maintains its integrity. The distinct yielding behavior of MAAc/NVI hydrogels at a low strain also indicates the fracture of the highly cross-linked aggregates formed via ionic H-bonds, which are responsible for the toughness improvement as compared to the AAc/NVI ones.

MAAc/NVP versus AAm/NVP. Pyrrolidone group pendant to hydrophilic polymer chains are known to form cooperative H-bonds in aqueous solutions with carboxylic

https://doi.org/10.1021/acs.macromol.2c01469
Macromolecules 2022, 55, 10576–10589

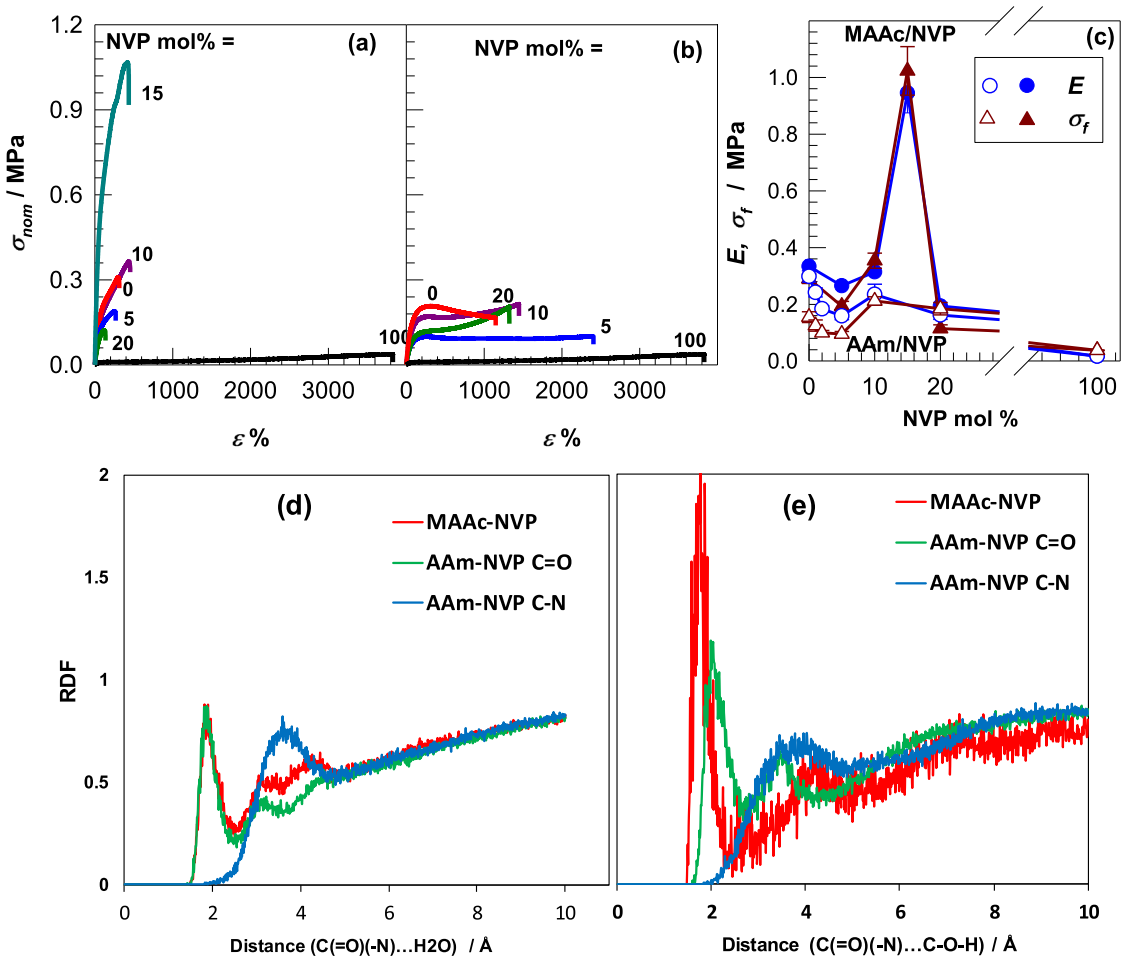

Figure 10. (a,b) Stress−strain curves of MAAc/NVP (a) and AAm/NVP hydrogels (b) at various compositions. (c) Young's modulus E and the fracture stress σ_f of MAAc/NVP and AAm/NVP hydrogels at various NVP mol %. (d,e) RDFs of polymer−water (d) and polymer−polymer interactions (e) of AAm/NVP and MAAc/NVP hydrogels at the critical comonomer ratio.

acid or amide groups.[24,49] In this section, NVP was copolymerized with MAAc and AAm monomers at various mole ratios. Figure 10a,b shows the stress−strain curves of MAAc/NVP (a) and AAm/NVP hydrogels (b), while Figure 10c compares their modulus E and fracture stress σ_f. AAm/NVP hydrogels exhibit poor mechanical properties over all compositions, while the MAAc/NVP hydrogel with 15 mol % NVP exhibits a peak in Young's modulus (0.95 ± 0.07 MPa) and fracture stress (1.0 ± 0.1 MPa), which are around 5-fold higher than those of AAm/NVP hydrogels (Figure 10c). The formation of a higher number of H-bonds in MAAc/NVP hydrogels was also reflected in their hysteresis energies U_{hys} (Figures S6 and S7). The U_{hys} of the first mechanical cycle of MAAc/NVP hydrogel at the critical composition, that is, at 15 mol % NVI, is 3 orders of magnitude higher than that of the corresponding AAm/NVP hydrogel (3750 ± 200 vs 62 ± 2 kJ·m^{-3}). A large fraction of the loading energy (78%) is dissipated in the former hydrogel, while it reduced to 25% in AAm/NVP hydrogel, reflecting a highly H-bonded structure of MAAc/NVP hydrogels.

The main difference between AAm/NVP and MAAc/NVP comonomer pairs is that their major components AAm and MAAc are the most hydrophilic and hydrophobic repeat units, respectively, with a significant difference in their log P/SA values, among all monomers studied (Figure 1B). Thus, the hydrophobicity of the major MAAc component seems to be one of the factors strengthening H-bonding interactions in MAAc/NVP hydrogels as compared to the AAm/NVP ones. Moreover, RDFs reveal that, although both hydrogels exhibit comparable polymer−water interactions, polymer−polymer interactions are much stronger for MAAc/NVP hydrogels (Figure 10d,e). AAm units with bidentate amine groups show a higher hydrophilicity compared to the MAAc units, which leads to the weaker polymer−polymer interactions and hence to a more negative electrostatic energy and a lower vdW energy per atom. Thus, the higher hydrophobicity and the larger number of inter-chain H-bonds of MAAc//NVP copolymers in water together with the incompatibility of their components produce mechanically stronger hydrogels as compared to the AAm/NVP ones.

Roadmap toward Mechanically Robust Hydrogels. The above results show that the mechanical properties of the copolymer hydrogels can be widely controlled by altering the type and composition of the comonomer mixture. Because the hydrogels were prepared at a fixed polymer volume fraction ϕ_2^o (=0.40 assuming that the densities are unity) and temperature T, and the tensile tests were conducted at a fixed stretch rate, Young's modulus E of the hydrogels directly relates to their apparent cross-linking density υ_e by $E=3\upsilon_e RT\phi_2^o$, where R is the gas constant.[50,51] Figure 11 reveals that the modulus, that is, the strength of H-bonds, varies between 10^{-1} and 10^{1} MPa that can be tuned by the type of the monomers.

https://doi.org/10.1021/acs.macromol.2c01469
Macromolecules 2022, 55, 10576−10589

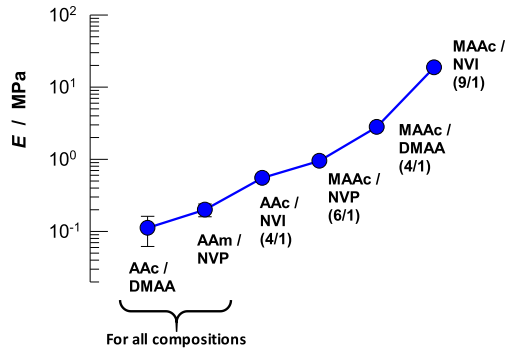

Figure 11. (a) Young's modulus E of the physical copolymer hydrogels with 60 wt % water. The molar ratio of the comonomers is given in parenthesis, while for AAc/DMAA and AAm/NVP hydrogels, the data are the average over all compositions.

AAc/DMAA and AAm/NVP hydrogels exhibit the lowest moduli, 0.11 ± 0.05 and 0.20 ± 0.04 MPa, respectively, over all comonomer compositions, while for all other comonomer pairs, the resulting hydrogels assume a maximum modulus at a critical composition. These compositions are also given in Figure 11 in parenthesis in terms of the molar ratio of the comonomers. MAAc and NVI are the most effective major and minor components, respectively, among the monomers we used to generate copolymer hydrogels with a high modulus and strength. Our results show that the crucial factors determining the mechanical performance of the copolymer hydrogels are the hydrophobicity of the major copolymer component, formation of H-bonds between ionic species, formation of strong H-bonded nanoaggregates during polymerization, and stronger and higher inter-chain H-bonding and hence electrostatic interactions. The interplay of these factors determines the maximum strength of inter-chain H-bonds at a critical composition deviating from 1/1. This deviation from 1/1 also suggests the existence of consecutive H-bond donor and acceptor monomer units on adjacent copolymer chains, facilitating cooperative hydrogen bonding. The number of consecutive units in the copolymer chains is hard to quantify for random copolymerization reactions, but it may be estimated from the reactivity ratios of the monomers. Although there is a large scatter in the reported monomer reactivity ratios,[52] the data show that both MAAc and AAc are more reactive than NVI in free-radical copolymerization, suggesting that the chains formed first will be richer in MAAc or AAc units. Similarly, MAAc is more reactive than both AAc and AAm.[52]

The calculated hydrophobicity of the six monomers studied in terms of log P/SA reveals that MAAc is the most hydrophobic monomer, while AAm, NVP, and DMAA are the least hydrophobic ones. Copolymer hydrogels with enhanced mechanical properties can be obtained when the copolymer chains are composed of hydrophobic major and hydrophilic minor monomer units, and the inter-chain H-bonding interactions are stronger than polymer−water interactions. Typical examples are MAAc/DMAA and MAAc/NVP hydrogels exhibiting a modulus in the range of MPa.

Because ionic H-bonds interconnecting the polymer chains are much stronger than typical H-bonds between the neutral molecules, the promotion of ionic H-bond between the monomers could be an alternative way to prepare high strength hydrogels. A hydrophobic microenvironment around the ionic H-bonds is also required to increase the bond strength as demonstrated using AAc/NVI and MAAc/NVI hydrogels. Replacing the AAc component with the hydrophobic MAAc in the copolymer hydrogel results in a 34-fold increase in the modulus (from 0.55 ± 0.05 to 18.7 ± 0.8 MPa) at their critical compositions.

Chemically cross-linked hydrogels formed by free-radical copolymerization are known to exhibit inhomogeneous distribution of cross-links due to the several nonidealities including different reactivities of the monomers, cyclization, and multiple cross-linking reactions.[53−56] Such spatial gel inhomogeneity results in the formation of regions of high polymer concentration (less swollen) surrounded by highly swollen regions of a low polymer concentration. A similar phenomenon seems to appear in mechanically strong H-bonded hydrogels, for example, in MAAc/DMAA and MAAc/NVI hydrogels. The appearance of a distinct yielding point and a significant mechanical hysteresis indicate the existence of strong H-bonded regions. MD simulations indeed show a transition from diluted to aggregated configuration as the mechanical properties of the hydrogel are improved. Unfavorable mixing energy of the hydrophobic monomer with both its comonomer and water also facilitates the formation of cooperativity in H-bonded aggregates. We should note that the significant improvement in the mechanical properties of MAAc/DMAA and MAAc/NVI hydrogels may also be related to the glassy state of H-bonded aggregates with low water content and high rigidity.[32,34] Thus, the strong H-bonded nanoaggregates break into fragments at the yield point while the weakly H-bonded regions maintain the hydrogel integrity, leading to toughness improvement.

The molecular weight of the copolymer chains and hence chain entanglements may also affect the strength of inter-chain H-bonds and hence the modulus E of the hydrogels.[24] This is because the higher the molecular weight, the larger the number of H-bonds between two copolymer chains and thus the stronger the cooperativity of H-bonds. To check this point, MAAc/DMAA, AAc/DMAA, MAAc/NVI, and AAc/NVI hydrogels at their critical compositions were solubilized in water as detailed in the Supporting Information. Comparison of the viscosities of 1 w/v % copolymer solutions in distilled water revealed that AAc-containing weak hydrogels exhibit higher viscosities than the MAAc-containing strong ones (Figure S8). Thus, the molecular weight difference of the hydrogels does not affect our results.

■ CONCLUSIONS

We presented the mechanical properties of six copolymer hydrogels by combining different monomeric units bearing H-bond donor and acceptor atoms. The hydrogel formation was achieved under the identical conditions by changing the type and molar ratio of the comonomers. By fixing one of the monomer type of the copolymer hydrogels while changing the second one, four sets of comparisons were made, which provided an important insight into the effect of the complex interplay between several energy components on the strength of H-bonds and hence the modulus of the hydrogels. The hydrophobicity of the monomers and the competing interactions between the copolymer chains and copolymer−water were quantitatively elucidated by the all-atom MD simulations in the explicit water, density functional theory calculations, and molecular descriptors by remaining faithful to the experimental compositions. The RDF plots enabled us to

https://doi.org/10.1021/acs.macromol.2c01469
Macromolecules 2022, 55, 10576−10589

differentiate the H-bonds formed between the copolymer chains, copolymer−water, and between the water molecules. The accurate calculations of the ratios of the electrostatic energy to total non-bonded energy made comparison of the total H-bond interactions of two different hydrogels possible. The calculated energies of mixing of the monomers in one another and the monomer hydrophobicity helped us to discuss the intercalation behavior of water molecules and phase separation phenomenon.

All the hydrogels could be dissolved in aqueous urea or alkaline solutions reflecting that they form via H-bonding interactions. The mechanical properties of the copolymer hydrogels can be widely controlled by altering the type and composition of the comonomer mixture. For instance, the modulus of the hydrogels varies between 10^{-1} and 10^{1} MPa that can be tuned by the type of the monomers. We also show that the enhancement in the modulus, mechanical strength, and toughness of the hydrogels can be monitored by conducting cyclic mechanical tests. A significant increase in the hysteresis energy predicts an internal fracture in the hydrogel and hence yielding phenomenon accompanied with toughness improvement.

The results show that the crucial factors determining the mechanical performance of the copolymer hydrogels are the hydrophobicity of the major copolymer component, formation of H-bonds between ionic species, formation of strong H-bonded nanoaggregates during polymerization, and stronger and higher inter-chain H-bonding and hence electrostatic interactions. MAAc and NVI are the most effective major and minor components, respectively, among the monomers we used, to generate copolymer hydrogels with a high modulus and strength. The calculated hydrophobicity of the monomers studied shows that MAAc is the most hydrophobic monomer, while AAm, NVP, and DMAA are the least hydrophobic ones. Copolymer hydrogels with enhanced mechanical properties can be obtained when the copolymer chains are composed of hydrophobic major and hydrophilic minor monomer units, and the inter-chain H-bonding interactions are stronger than polymer−water interactions. Typical examples are MAAc/DMAA and MAAc/NVP hydrogels exhibiting a modulus in the range of MPa. The formation of ionic H-bonds between the monomers in a hydrophobic microenvironment significantly improves the mechanical properties of the copolymer hydrogels as demonstrated by comparing AAc/NVI and MAAc/NVI hydrogels.

MD simulations reveal that the improvement in the mechanical properties is accompanied with a transition from diluted to aggregated configuration due to the unfavorable mixing energy of the hydrophobic monomer with both its comonomer and water facilitating the formation of cooperativity in H-bonded aggregates. Thus, the strong H-bonded nanoaggregates in the hydrogel break into fragments at the yield point while the weakly H-bonded regions maintain the hydrogel integrity, leading to a significant toughness improvement.

■ ASSOCIATED CONTENT

Supporting Information

The Supporting Information is available free of charge at https://pubs.acs.org/doi/10.1021/acs.macromol.2c01469.

Supplementary synthesis and characterization data including swelling, rheological, and mechanical test results and details of MD simulations (PDF)

■ AUTHOR INFORMATION

Corresponding Authors

Mine Yurtsever − *Department of Chemistry, Istanbul Technical University, 34469 Istanbul, Turkey;* orcid.org/0000-0001-6504-7182; Email: mine@itu.edu.tr

Oguz Okay − *Department of Chemistry, Istanbul Technical University, 34469 Istanbul, Turkey;* orcid.org/0000-0003-2717-4150; Email: okayo@itu.edu.tr

Authors

Cagla Erkoc − *Department of Chemistry, Istanbul Technical University, 34469 Istanbul, Turkey*

Erol Yildirim − *Department of Chemistry, Middle East Technical University, 06800 Ankara, Turkey;* orcid.org/0000-0002-9989-9882

Complete contact information is available at: https://pubs.acs.org/10.1021/acs.macromol.2c01469

Author Contributions

The manuscript was written through contributions of all authors. All authors have given approval to the final version of the manuscript.

Notes

The authors declare no competing financial interest.

■ ACKNOWLEDGMENTS

C.E. thanks TUBITAK BIDEB 118C113 project for a PhD scholarship. O.O. thanks the Turkish Academy of Sciences (TUBA) for the partial support. M.Y. acknowledges the computer time provided by the National High Performance Computing Center (UHEM) under grant number 5004452017.

■ REFERENCES

(1) Creton, C. 50th Anniversary Perspective: Networks and Gels: Soft but Dynamic and Tough. *Macromolecules* **2017**, *50*, 8297−8316.

(2) Gong, J. P.; Katsuyama, Y.; Kurokawa, T.; Osada, Y. Double-network hydrogels with extremely high mechanical strength. *Adv. Mater.* **2003**, *15*, 1155−1158.

(3) Webber, R. E.; Creton, C.; Brown, H. R.; Gong, J. P. Large Strain Hysteresis and Mullins Effect of Tough Double-Network Hydrogels. *Macromolecules* **2007**, *40*, 2919−2927.

(4) Annabi, N.; Tamayol, A.; Uquillas, J. A.; Akbari, M.; Bertassoni, L. E.; Cha, C.; Camci-Unal, G.; Dokmeci, M. R.; Peppas, N. A.; Khademhosseini, A. 25th Anniversary Article: Rational Design and Applications of Hydrogels in Regenerative Medicine. *Adv. Mater.* **2014**, *26*, 85−124.

(5) Cui, K.; Gong, J. P. Aggregated Structures and Their Functionalities in Hydrogels. *Aggregate* **2021**, *e33*(). DOI: 10.1002/agt2.33

(6) Fan, H.; Gong, J. P. Fabrication of Bioinspired Hydrogels: Challenges and Opportunities. *Macromolecules* **2020**, *53*, 2769−2782.

(7) Mredha, Md. T. I.; Jeon, I. Biomimetic Anisotropic Hydrogels: Advanced Fabrication Strategies, Extraordinary Functionalities, and Broad Applications. *Prog. Mater. Sci.* **2022**, *124*, 100870.

(8) Chirani, N.; Yahia, L.; Gritsch, L.; Motta, F. L.; Chirani, S.; Faré, S. History and Applications of Hydrogels. *J. Biomed. Sci.* **2015**, *4*, 1−23.

(9) De France, K. J.; Xu, F.; Hoare, T. Structured Macroporous Hydrogels: Progress, Challenges, and Opportunities. *Adv. Healthcare Mater.* **2018**, *7*, 1700927.
(10) Zhao, X.; Chen, X.; Yuk, H.; Lin, S.; Liu, X.; Parada, G. Soft Materials by Design: Unconventional Polymer Networks Give Extreme Properties. *Chem. Rev.* **2021**, *121*, 4309−4372.
(11) Qiao, Z.; Cao, M.; Michels, K.; Hoffman, L.; Ji, H.-F. Design and Fabrication of Highly Stretchable and Tough Hydrogels. *Polym. Rev.* **2020**, *60*, 420−441.
(12) Gong, J. P. Why are Double Network Hydrogels So Tough? *Soft Matter* **2010**, *6*, 2583−2590.
(13) Liu, Y.; Hsu, S.-H. Synthesis and Biomedical Applications of Self-Healing Hydrogels. *Front. Chem.* **2018**, *6*, 449.
(14) Wei, Z.; Yang, J. H.; Zhou, J.; Xu, F.; Zrínyi, M.; Dussault, P. H.; Osada, Y.; Chen, Y. M. Self-Healing Gels Based on Constitutional Dynamic Chemistry and Their Potential Applications. *Chem. Soc. Rev.* **2014**, *43*, 8114−8131.
(15) Talebian, S.; Mehrali, M.; Taebnia, N.; Pennisi, C. P.; Kadumudi, F. B.; Foroughi, J.; Hasany, M.; Nikkhah, M.; Akbari, M.; Orive, G.; Dolatshahi-Pirouz, A. Self-Healing Hydrogels: The Next Paradigm Shift in Tissue Engineering? *Adv. Sci.* **2019**, *6*, 1801664.
(16) Okay, O. How to Design both Mechanically Strong and Self-Healable Hydrogels? *Adv. Polym. Sci.* **2020**, *285*, 21−62.
(17) Taylor, D. L.; in het Panhuis, M. het Panhuis, M. Self-Healing Hydrogels. *Adv. Mater.* **2016**, *28*, 9060−9093.
(18) Voorhaar, L.; Hoogenboom, R. Supramolecular Polymer Networks: Hydrogels and Bulk Materials. *Chem. Soc. Rev.* **2016**, *45*, 4013−4031.
(19) You, Y.; Yang, J.; Zheng, Q.; Wu, N.; Lv, Z.; Jiang, Z. Ultra-Stretchable Hydrogels with Hierarchical Hydrogen Bonds. *Sci. Rep.* **2020**, *10*, 11727.
(20) Dai, X.; Zhang, Y.; Gao, L.; Bai, T.; Wang, W.; Cui, Y.; Liu, W. A Mechanically Strong, Highly Stable, Thermoplastic, and Self-Healable Supramolecular Polymer Hydrogel. *Adv. Mater.* **2015**, *27*, 3566−3571.
(21) Gao, H.; Wang, N.; Hu, X.; Nan, W.; Han, Y.; Liu, W. Double Hydrogen-Bonding pH-Sensitive Hydrogels Retaining High-Strengths Over a Wide pH Range. *Macromol. Rapid Commun.* **2013**, *34*, 63−68.
(22) Guo, M.; Pitet, L. M.; Wyss, H. M.; Vos, M.; Dankers, P. Y. W.; Meijer, E. W. Tough Stimuli-Responsive Supramolecular Hydrogels with Hydrogen-Bonding Network Junctions. *J. Am. Chem. Soc.* **2014**, *136*, 6969−6977.
(23) Jeon, I.; Cui, J.; Illeperuma, W. R. K.; Aizenberg, J.; Vlassak, J. J. Extremely Stretchable and Fast Self-Healing Hydrogels. *Adv. Mater.* **2016**, *28*, 4678−4683.
(24) Song, G.; Zhang, L.; He, C.; Fang, D.-C.; Whitten, P. G.; Wang, H. Facile Fabrication of Tough Hydrogels Physically Cross-Linked by Strong Cooperative Hydrogen Bonding. *Macromolecules* **2013**, *46*, 7423−7435.
(25) Song, G.; Zhao, Z.; Peng, X.; He, C.; Weiss, R. A.; Wang, H. Rheological Behavior of Tough PVP-in Situ-PAAm Hydrogels Physically Cross-Linked by Cooperative Hydrogen Bonding. *Macromolecules* **2016**, *49*, 8265−8273.
(26) Chang, X.; Geng, Y.; Cao, H.; Zhou, J.; Tian, Y.; Shan, G.; Bao, Y.; Wu, Z. L.; Pan, P. Dual-Crosslink Physical Hydrogels with High Toughness Based on Synergistic Hydrogen Bonding and Hydrophobic Interactions. *Macromol. Rapid Commun.* **2018**, *39*, No. e1700806.
(27) Hu, X.; Vatankhah-Varnoosfaderani, M.; Zhou, J.; Li, Q.; Sheiko, S. S. Weak Hydrogen Bonding Enables Hard, Strong, Tough, and Elastic Hydrogels. *Adv. Mater.* **2015**, *27*, 6899−6905.
(28) Zhang, X. N.; Wang, Y. J.; Sun, S.; Hou, L.; Wu, P.; Wu, Z. L.; Zheng, Q. A Tough and Stiff Hydrogel with Tunable Water Content and Mechanical Properties Based on the Synergistic Effect of Hydrogen Bonding and Hydrophobic Interaction. *Macromolecules* **2018**, *51*, 8136−8146.
(29) Zhou, Q.; Yang, K.; He, J.; Yang, H.; Zhang, X. A Novel 3D-Printable Hydrogel with High Mechanical Strength and Shape Memory Properties. *J. Mater. Chem. C* **2019**, *7*, 14913−14922.
(30) Zhang, X. N.; Du, C.; Wei, Z.; Du, M.; Zheng, Q.; Wu, Z. L. Stretchable Sponge-like Hydrogels with a Unique Colloidal Network Produced by Polymerization-Induced Microphase Separation. *Macromolecules* **2022**, *55*, 1424−1434.
(31) Su, E.; Yurtsever, M.; Okay, O. A Self-Healing and Highly Stretchable Polyelectrolyte Hydrogel via Cooperative Hydrogen-Bonding as a Superabsorbent Polymer. *Macromolecules* **2019**, *52*, 3257−3267.
(32) Zhang, X. N.; Du, C.; Du, M.; Zheng, Q.; Wu, Z. L. Kinetic Insights into Glassy Hydrogels with Hydrogen Bond Complexes as the Cross-Links. *Mater. Today Phys.* **2020**, *15*, 100230.
(33) Ding, H.; Zhang, X. N.; Zheng, S. Y.; Song, Y.; Wu, Z. L.; Zheng, Q. Hydrogen Bond Reinforced Poly(1-vinylimidazole-co-acrylic acid) Hydrogels with High Toughness, Fast Self-Recovery, and Dual pH-Responsiveness. *Polymer* **2017**, *131*, 95−103.
(34) Du, C.; Zhang, X. N.; Sun, T. L.; Du, M.; Zheng, Q.; Wu, Z. L. Hydrogen-Bond Association-Mediated Dynamics and Viscoelastic Properties of Tough Supramolecular Hydrogels. *Macromolecules* **2021**, *54*, 4313−4325.
(35) Akar, I.; Foster, J. C.; Leng, X.; Pearce, A. K.; Mathers, R. T.; O'Reilly, R. K. Log P_{oct}/SA Predicts the Thermoresponsive Behavior of P(DMA-co-RA) Statistical Copolymers. *ACS Macro Lett.* **2022**, *11*, 498−503.
(36) Means, A. K.; Grunlan, M. A. Modern Strategies To Achieve Tissue-Mimetic, Mechanically Robust Hydrogels. *ACS Macro Lett.* **2019**, *8*, 705−713.
(37) *MS 5.0*, Accelrys Software Inc., San Diego, USA, 2009.
(38) MacDonald, J. C.; Dorrestein, P. C.; Pilley, M. M. Design of Supramolecular Layers via Self-Assembly of Imidazole and Carboxylic Acids. *Cryst. Growth Des.* **2001**, *1*, 29−38.
(39) Sun, H. COMPASS: An ab Initio Forcefield Optimized for Condensed-Phase Applications - Overview with Details on Alkane and Benzene Compounds. *J. Phys. Chem. B* **1998**, *102*, 7338−7364.
(40) Sun, H.; Ren, P.; Fried, J. R. The COMPASS Forcefield: Parameterization and Validation for Polyphosphazenes. *Comput. Theor. Polym. Sci.* **1998**, *8*, 229−246.
(41) Fan, C. F.; Olafson, B. D.; Blanco, M.; Hsu, S. L. Application of Molecular Simulation to Derive Phase Diagrams of Binary Mixtures. *Macromolecules* **1992**, *25*, 3667−3676.
(42) Steinbrecher, T.; Joung, I. S.; Case, D. A. Soft-Core Potentials in Thermodynamic Integration. Comparing One- and Two-Step Transformations. *J. Comp. Chem.* **2011**, *32*, 3253−3263.
(43) Ghose, A. K.; Viswanadhan, V. N.; Wendoloski, J. J. Prediction of Hydrophobic (Lipophilic) Properties of Small Organic Molecules using Fragmental Methods: An Analysis of ALOGP and CLOGP Methods. *J. Phys. Chem. A.* **1998**, *102*, 3762−3772.
(44) Stanton, D. T.; Jurs, P. C. Development and Use of Charged Partial Surface Area Structural Descriptors in Computer-Assisted Quantitative Structure-Property Relationship Studies. *Anal. Chem.* **1990**, *62*, 2323−2329.
(45) Anufrieva, E. V.; Birshtein, T. M.; Nekrasova, T. N.; PtitsynSheveleva, O. B. T. V. The Models of the Denaturation of Globular Proteins. II. Hydrophobic Interactions and Conformational Transition in Polymethacrylic Acid. *J. Polym. Sci. C* **1968**, *16*, 3519−3531.
(46) Oyama, H. T.; Tang, W. T.; Frank, C. W. Effect of the Hydrophobic Interaction in the Poly(methacrylic acid)/Pyrene End-Labeled Polyethylene glycol) Complex. *Macromolecules* **1987**, *20*, 1839−1847.
(47) Callear, S. K.; Hursthouse, M. B.; Threlfall, T. L. A Systematic Study of the Crystallisation Products of a Series of Dicarboxylic Acids with Imidazole Derivatives. *CrystEngComm* **2010**, *12*, 898−908.
(48) Meot-Ner, M. The Ionic Hydrogen Bond. *Chem. Rev.* **2005**, *105*, 213−284.
(49) Bimendina, L. A.; Roganov, V. V.; Bekturov, E. E. Hydrodynamic Properties of Complexes of Polymethacrylic Acid -

https://doi.org/10.1021/acs.macromol.2c01469
Macromolecules 2022, 55, 10576−10589

Polyvinylpyrrolidone in Solutions. *J. Polym. Sci. Polym. Symp.* **1974**, *44*, 65−74.
(50) Mark, J. E.; Erman, B. *Rubberlike Elasticity*; Cambridge University Press: Cambridge, U.K.., 2007.
(51) Treloar, L. R. G. *The Physics of Rubber Elasticity*; University Press: Oxford, 1975.
(52) *Polymer Handbook*, Brandrup, J.; Immergut, E. H.; Grulke, E. A., Eds.; John Wiley, New York, 4th ed., 1999, pp II/182-II/285.
(53) Bastide, J.; Candau, S. J. *Structure of Gels as Investigated by Means of Static Scattering Techniques*, editor. In *Physical Properties of Polymeric Gels*; Cohen Addad, J. P., Ed.: New York: Wiley; 1996. p. 143.
(54) Shibayama, M. Spatial inhomogeneity and dynamic fluctuations of polymer gels. *Macromol. Chem. Phys.* **1998**, *199*, 1−30.
(55) Funke, F.; Okay, O.; Joos-Muller, B. Microgels: Intramolecularly Crosslinked Macromolecules with a Globular Structure. *Adv. Polym. Sci.* **1998**, *136*, 139−234.
(56) Kizilay, M. Y.; Okay, O. Effect of Initial Monomer Concentration on Spatial Inhomogeneity in Poly(acrylamide) Gels. *Macromolecules* **2003**, *36*, 6856−6862.

https://doi.org/10.1021/acs.macromol.2c01469
Macromolecules 2022, 55, 10576−10589